Environ. Sci. Technol. **2006**, *40,* 6044−6050

Inverse Characterization of NAPL Source Zones

MARK A. NEWMAN,*,† KIRK HATFIELD,† JOEL HAYWORTH,‡ P. SURESH C. RAO,§ AND TOM STAUFFER‡

Department of Civil and Coastal Engineering, University of Florida, P.O. Box 116580, Gainesville, Florida 32611-6450, Air Force Research Laboratory, Tyndall AFB, Florida, and School of Civil Engineering, Purdue University, West Lafayette, Indiana

This work presents a possible tool for inverse characterization of NAPL (nonaqueous phase liquid) source zones in terms of contaminant mass flux. A hybrid solution technique was applied that considers contaminant transport through a vertical flux plane. The hybrid solution technique takes advantage of the robust solution capabilities of simulated annealing (SA) and the uncertainty estimation capabilities of minimum relative entropy (MRE). The coupled technique (SA-MRE) provides probability density functions and confidence intervals that would not be available from an independent SA algorithm, and they are obtained more efficiently than if provided by an independent MRE algorithm. The SA-MRE method was used to characterize a NAPL source zone that was emplaced in a three-dimensional aquifer model. When dissolution experiments were complete, the aquifer model was excavated, and the distribution of NAPL zones was recorded using digital images of excavation grids. The excavation images were compiled into a three-dimensional representation of the source zone for comparison with and validation of modeling results.

Introduction

Contaminant source characterization represents solution of an inverse problem and is usually considered within an optimization framework (*1*). Various optimization methodologies have been applied for the purpose of source characterization (*2*−*12*). When formulating the inverse problem, one must consider how to represent or "characterize" the source. For this study the source zone is characterized in terms of mass flux, where flux refers to the mass of water and or contaminants flowing through a specified control plane (cross-sectional area) during a given period of time. The units associated with mass flux are $M/(L^2T)$ where the terms M, L, and T represent the base units of mass, length, and time, respectively. The benefits of flux-based characterization are discussed by Rao et al. (*13*).

The purpose of the work presented here is to provide a tool for characterizing NAPL source zones based upon observed contaminant concentration data. Many previous studies (*1*, *2*, *5*, *6*, *8*−*10*, *12*) have considered source location problems based upon a horizontal discretization of the system and attempted to locate sources by choosing from a discrete set of possible source locations of which the actual source location was a subset. The primary difference in this work is the application of SA-MRE, a hybrid solution technique (*21*), to estimate NAPL flux through a vertical flux plane. The SA-MRE method was developed to take advantage of the random search capabilities of simulated annealing (SA) and the uncertainty estimation capabilities of minimum relative entropy (MRE) (*21*). The coupled technique is capable of converging more efficiently than MRE and provides probability density functions and confidence intervals that are not available from an independent SA algorithm. Another unique aspect is that this work provides comparison of model-simulated results with experimentally observed source zone excavation data in order to verify the inverse model results.

It should be noted that multicomponent NAPL dissolution is a complex process. Several studies have been performed (*4*, *14*−*20*) in order to investigate what actually occurs as multicomponent NAPL sources dissolve. However, because this work is the first application of the SA-MRE flux plane model to a NAPL source problem, a simplified approach was considered. The flux plane model used here is only applicable for characterization of source zones and plumes exhibiting apparent steady-state dissolution conditions. It is acknowledged that for multicomponent NAPL dissolution the source composition will change over time as the components of higher solubility dissolve faster (*15*, *16*) and that neglecting the corresponding changes in nonaqueous phase activity coefficients may introduce prediction errors. However, for this study ideal steady-state dissolution is assumed. It is acknowledged that ideal steady-state dissolution can only occur for mixtures containing components of similar structure and solubility. The application envisioned for this study represents cases in which a source zone is discovered long after the contaminants were introduced into the subsurface. Under such conditions, what is often observed is the tail end of the dissolution process, and the dissolution process may appear steady for extended periods of time.

Materials and Methods

Aquifer Model. NAPL dissolution experiments were performed in a three-dimensional aquifer model constructed at the Air Force Research Laboratory, Tyndall Air Force Base, FL. The system was designed for use with chlorinated solvents; all wetted surfaces were stainless steel or glass, minimizing the partitioning of hydrophobic chemicals to system components. All liquid effluent and vapor streams passed through physical and/or chemical traps, eliminating exposure to hazardous chemicals and allowing quantitative mass balance determinations. In the experiment performed for this study, the model was configured to simulate a homogeneous unconfined aquifer. The physical, hydrodynamic, and transport characteristics of the system are presented in Table 1 and are discussed in greater detail by Newman et al. (*21*, *22*).

NAPL Dissolution Experiment. The NAPL dissolution experiment for this study was started by establishing steady flow with an average saturated thickness (h_s) of 0.922 m, and an average pore water velocity of 0.34 m/day (corresponding to an average effluent water flowrate (Q_x) of 0.047 m^3/day and a specific discharge (q_x) of 0.102 m/day). Once steady flow was established, ten NAPL sources, each composed of a mixture of 55% *n*-hexadecane and 45% perchloroethene (PCE) by volume, were emplaced within the up-gradient region of the flow system by slow injection of a known volume (10 mL for each source). The corresponding mole fractions

* Corresponding author phone: (352)392-9537; fax (352)392-3394; e-mail: markn@ce.ufl.edu.
† University of Florida.
‡ Air Force Research Laboratory, Tyndall AFB.
§ Purdue University.

10.1021/es060437s CCC: $33.50

Published on Web 08/29/2006

TABLE 1. Physical, Hydraulic, and Transport Properties of the Three-Dimensional Aquifer Model (Newman, 2001)

parameter	value
porous media	Flint Silica #14 (U.S. Silica, Ottawa, IL)
porous media dimensions (length × width × height; m)	2.0 × 0.5 × 1.0
median grain size (d_{50}; m)	0.0012
porosity (n)	0.3
longitudinal dispersivity (α_L; m)	0.002
transverse dispersivity (α_T; m)	0.0002

TABLE 2. System Parameters for the Multiple Source NAPL Experiment

source	source location (x, y, z; m)	volume (mL)
1	0.50, 0.15, 0.75	10.78
2	0.50, 0.20, 0.70	11.78
3	0.50, 0.25, 0.65	10.45
4	0.50, 0.30, 0.60	10.44
5	0.50, 0.25, 0.55	10.15
6	0.80, 0.25, 0.65	10.44
7	0.80, 0.30, 0.60	10.44
8	0.80, 0.25, 0.55	10.44
9	0.80, 0.15, 0.45	10.44
10	0.80, 0.10, 0.40	10.44

were 0.3 for n-hexadecane and 0.7 for PCE. The NAPL solution also contained the hydrophobic dye oil red-O. Source conditions are summarized in Table 2, and the source locations are shown in Figure 1. It should be noted that n-hexadecane is a light nonaqueous phase liquid (LNAPL) with a density ($\rho_{n-\text{hexa}} = 0.7733$ g/mL) less than that of water ($\rho_w = 1.00$ g/mL). In order to ensure that the NAPL mixture behaved as a dense nonaqueous phase liquid (DNAPL) the solution was prepared so that the multicomponent NAPL was denser than water ($\rho_{NAPL} = 1.16$ g/mL).

The n-hexadecane was included in the NAPL solution for two reasons: to prolong the dissolution time of the PCE sources and, with the combination of oil red-O dye, to provide a visual indicator of the source zone distribution to be recorded during excavation of the aquifer model. n-Hexadecane is a hydrophobic compound with an extremely low aqueous solubility ($S_{n-\text{hexa}} = 3.588 \times 10^{-3}$ mg/L). Including a hydrophobic compound in the NAPL mixture provides a partitioning media for PCE which acts to reduce the effective solubility of PCE and increases the lifetime of the PCE sources. The dissolution of a multicomponent NAPL is described using the aqueous analog of Raoult's law for the vapor pressure of a solution

$$S^e_{i(w)} = X_{i(N)} S^o_{i(w)} \quad (1)$$

where $X_{i(N)}$ is the mole fraction of component i in the NAPL mixture, $S_{i(w)}$ is the pure aqueous solubility of NAPL component i, and $S^e_{i(w)}$ is the resulting effective aqueous solubility of component i.

Pankow and Cherry (*23*) observed that there are a wide range of aqueous solubility limits reported in the literature for chlorinated solvents such as PCE and TCE. A review of the literature found that the aqueous solubility of PCE is reported to range between 149 mg/L (*24*) and 200 mg/L (*25*). For a NAPL composition by volume of 45% PCE and 55% n-hexadecane, the range of reported PCE solubility limits can be used with eq 1 to estimate the expected experimental range of effective solubility for PCE. The result is that the maximum expected aqueous phase PCE concentration should be within 105−140 mg/L.

The second benefit of including n-hexadecane is that it is essentially insoluble in water and acts as a nonwetting phase when injected into the porous medium. The nonwetting n-hexadecane gets trapped as blobs or globules by capillary forces within the pores (*26*), and because it is insoluble in water it remains in place marking the extent of

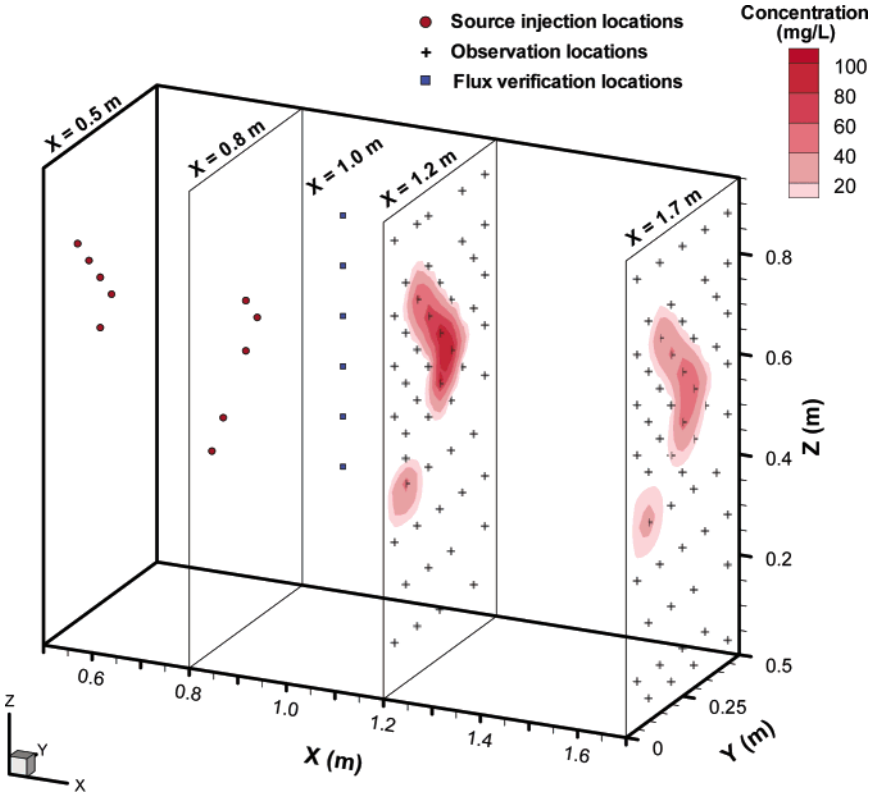

FIGURE 1. Steady-state three-dimensional PCE concentration distribution for day 44.

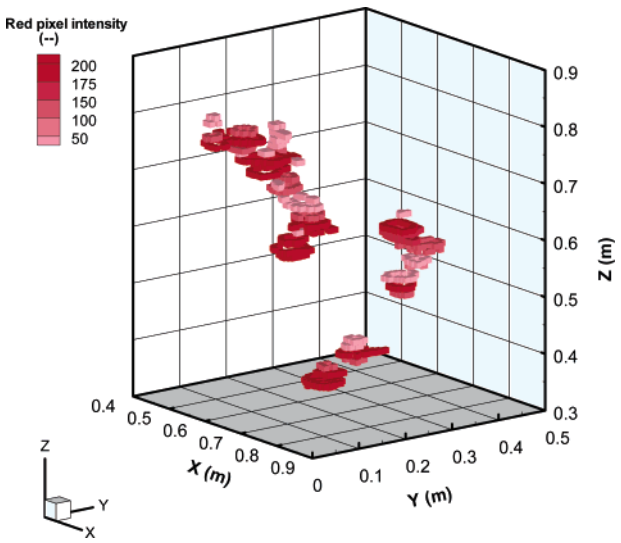

FIGURE 2. Three-dimensional representation of DNAPL source zone based upon digital excavation photographs. (The color shown represents the observed red pixel intensity in the excavation photographs.)

the initial source zone distribution. The hydrophobic dye, oil red-O, will partition preferentially into the *n*-hexadecane, thus providing a visual indication of the NAPL source zone spatial distribution.

Aqueous phase PCE concentrations were collected within the aquifer model during the transient stage of plume development and over an extended time period (approximately 1 month) in which the plume was essentially at steady state. During the steady-state period, PCE concentrations were collected as shown in Figure 1, which represents the observed PCE concentration distribution for day 44 of the dissolution experiment. Upon completion of the dissolution experiment the porous media was excavated, and the source zone distribution delineated by oil red-O dye was recorded using excavation grids and digital images. The digital images were compiled to develop a three-dimensional representation of the NAPL source zone (Figure 2) for comparison with modeling results.

Modeling

Flux Plane Model. The flux plane model as presented by Newman et al. (*21*) was developed for uniform horizontal flow with conservative, advective-dispersive transport in a homogeneous aquifer. It is assumed that contaminant concentrations are measured at multiple locations downgradient of a contaminant source zone and that a flux plane is located between the contaminant source zone and the downgradient observation locations. The flux plane is represented numerically by dividing the plane into N rectangular elements each having a flux component m_n. The total mass flux through the plane is the sum of the N elemental fluxes, and the resulting concentration (C_j) at location j has a component contributed from each of the elemental fluxes m_n.

$$C_j = \sum_{n=1}^{N} g_{jn} m_n \tag{2}$$

The term g_{jn} is a steady-state transfer function which was derived from an analytical solution for advective-dispersive transport developed by Domenico and Robbins (*27*)

$$g_{jn} = \frac{1}{4q_x}\left\{\mathrm{erf}\left[\frac{y'_n + b}{2(\alpha_y x'_n)^{1/2}}\right] - \mathrm{erf}\left[\frac{y'_n - b}{2(\alpha_y x'_n)^{1/2}}\right]\right\}\left\{\mathrm{erf}\left[\frac{z'_n + d}{2(\alpha_z x'_n)^{1/2}}\right] - \mathrm{erf}\left[\frac{z'_n - d}{2(\alpha_z x'_n)^{1/2}}\right]\right\} \tag{3}$$

where q_x is the specific discharge [L/T]; erf represents the error function; b and d represent the half-width and half-height of a flux plane element; α_x, α_y, and α_z represent the dispersivity components [L] along the x, y, and z-axes; and x'_n, y'_n, and z'_n are the relative coordinates as defined by Newman et al. (*21*). It should be noted that due to the steady-state assumption there is no retardation term in the transfer function (eq 3) and that the lateral and vertical extents of the plume are determined primarily by the transverse dispersivities α_y and α_z.

It is acknowledged that incorporating a numerical solution rather than an analytical solution could expand the applicability of the flux plane model. But development and

TABLE 3. Simulated Flux at the Intermediate Flux Planes for Days 44 and 58 of the Multiple-Source PCE Dissolution Experiment

observation coordinates					day 44 SA-MRE		day 58 SA-MRE	
X	*Y*	*Z*	obsd PCE concn (mg/L)	calcd flux mg (cm² day)	simulated flux mg (cm² day)	percent difference	simulated flux mg (cm² day)	percent difference
1.10	0.25	0.85	0.39	0.00	0.00		0.00	
1.10	0.25	0.75	0.38	0.00	0.00		0.00	
1.10	0.25	0.65	102.04	1.04	0.93	11%	0.93	11%
1.10	0.25	0.55	81.33	0.83	0.84	−1%	0.84	−1%
1.10	0.25	0.45	1.52	0.02	0.01	0	0.01	
1.10	0.25	0.35	0.45	0.00	0.00		0.00	
1.00	0.25	0.85	0.37	0.090	0.00		0.00	
1.00	0.25	0.75	0.30	0.00	0.00		0.01	
1.00	0.25	0.65	106.07	1.08	1.06	2%	1.05	3%
1.00	0.25	0.55	112.76	1.15	1.13	2%	1.00	13%
1.00	0.25	0.45	1.86	0.02	0.01		0.01	
1.00	0.25	0.35	0.51	0.01	0.00		0.00	
0.90	0.25	0.85	0.35	0.00	0.00		0.00	
0.90	0.25	0.75	0.33	0.00	0.00		0.00	
0.90	0.25	0.65	111.01	1.13	1.18	−4%	1.10	3%
0.90	0.25	0.55	117.46	1.20	1.17	2%	1.17	2%
0.90	0.25	0.45	1.75	0.02	0.01		0.00	
0.90	0.25	0.35	0.49	0.01	0.00		0.00	
		mean absolute error			0.017		0.023	
		average run time (min)			10		10	

TABLE 4. Simulated Flux at the Source Planes for Days 44 and 58 of the Multiple-Source PCE Dissolution Experiment

effective PCE solubility	
upper limit (mg/L)	lower limit (mg/L)
140	105

calculated effective flux	
upper limit mg/(cm^2 day)	lower limit mg/(cm^2 day)
1.43	1.07

observation coordinates			day 44 SA-MRE simulated flux mg (cm^2 day)	day 58 SA-MRE simulated flux mg (cm^2 day)
X	*Y*	*Z*		
0.80	0.25	0.65	1.40	1.36
0.80	0.30	0.60	1.44	1.40
0.80	0.25	0.55	1.30	1.25
0.80	0.15	0.45	0.01	0.01
0.80	0.10	0.40	0.74	0.75
av run time (min)			10	11

implementation of a numerical model requires a greater amount of prior information, and such information is not always readily available. By reducing the amount of requisite information the flux plane method provides a simple tool that can be used for preliminary assessment of a contaminant site when very little information is typically known about the flow field and source characteristics.

Hybrid SA-MRE Model. The hybrid SA-MRE method combines two optimization techniques: simulated annealing (SA) and minimum relative entropy (MRE) (*21*). Random search techniques such as SA have two advantages: they require only objective function information to determine convergence, so derivative calculations are not required; and they implement probabilistic transition rules, which allow them to avoid local minima in order to move toward a global minimum (*28*−*31*). However, a typical drawback of random search techniques is that although theoretically they should locate a "global" optimum provided an adequate number of perturbations, the reliability of the final estimates are not always readily verified.

MRE is a gradient-based optimization technique capable of using observation data to infer probability density functions and expected values for unknown model variables (*32*−*35*). As the term implies, gradient-based optimization methods are dependent upon calculating objective function derivatives (gradients). Gradient-based methods are very efficient at finding a local minimum when the gradient is steep and are usually most efficient once in the general neighborhood of the global optimum. But, for cases where the minimum exists in an area with a shallow gradient or where there are numerous local minima, gradient-based methods often have problems converging. The hybrid (SA-MRE) solution technique was developed in order to take advantage of the robust solution capabilities of SA and the uncertainty estimation capabilities of MRE.

Model Application. The flux plane inverse model was used to estimate the magnitude and distribution of PCE mass flux from the system of NAPL sources emplaced in the laboratory aquifer model. The aqueous-phase PCE concentrations measured downgradient of the DNAPL source zones at location $x = 1.7$ m and $x = 1.2$ m were used as the observed contaminant concentrations. The goal was to estimate the PCE mass flux at three intermediate flux planes ($x = 1.10$ m, $x = 1.00$ m, and $x = 0.90$ m) and at the downgradient edge of the source zone ($x = 0.8$ m) (Figure 1). The simulated flux values at the intermediate flux planes were verified using experimentally calculated flux values based upon observed concentrations. The simulated flux values at the source plane were verified by comparison of the model simulated values to values estimated by assuming a constant specific discharge and aqueous NAPL saturation at the flux plane. It is acknowledged that the assumption of NAPL saturation is an overestimation, as NAPL saturation levels are actually only expected to occur at the NAPL−water interfaces. The spatial distribution of PCE mass flux at the source plane was verified by comparison to the three-dimensional source zone distribution recorded during excavation of the aquifer model.

The vertical flux plane for this application was established as a grid consisting of 720 flux cells each of which was a 2-cm square plane source with a possible source intensity ranging from a lower value of 0 mg/L to a specified upper limit. For this case, the pure phase upper solubility limit for PCE (200 mg/L) was used to determine the simulated flux upper limit (2.04 mg/(cm^{2}day)) for the flux plane model.

With the flux plane and parameter limits established the search area was segregated following the same procedure as Newman et al. (*21*). The flux grid was superimposed on the observed PCE concentration distribution from the furthest observation plane ($x = 1.7$ m). The 25-mg/L contour was

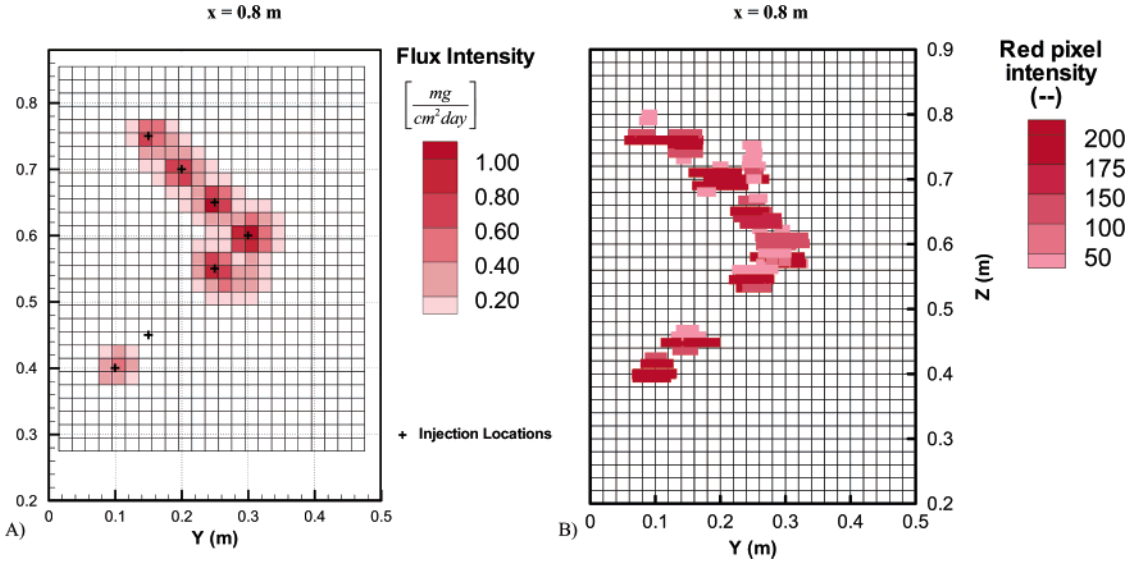

FIGURE 3. (A) SA-MRE simulated flux at the PCE source plane (day 44) and (B) DNAPL source zone distribution recorded during excavation.

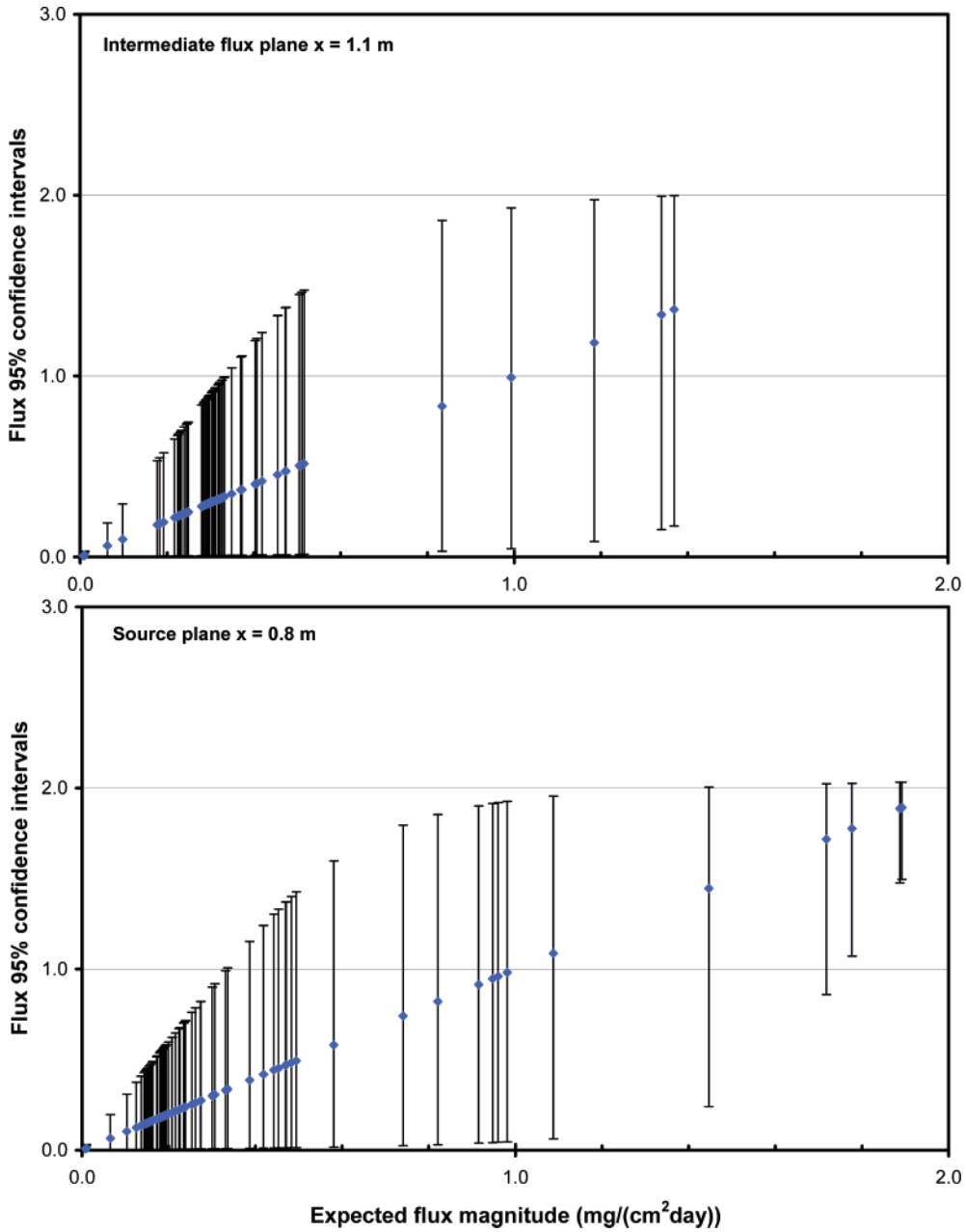

FIGURE 4. Simulated mean (expected) flux values and 95% confidence intervals for the intermediate flux plane (x = 1.1 m) and (x = 0.8 m).

then used as the segregation contour, and the initial model input values were established. All flux cells that were outside of the segregated area were given an initial value of 0.1 mg/(cm^2 day).

Using a convergence criteria of 1e-6, a maximum number of iterations of 90,000, and 44 downgradient concentration observations (22 each at observation planes x = 1.2 m and x = 1.7 m) the SA-MRE model was applied to estimate the PCE mass flux at three intermediate flux planes (x = 0.9 m, x = 1.0 m, x = 1.1 m) and at the downgradient edge of the source zone (x = 0.8 m). The results are discussed in the following section.

Results and Discussion

Model Verification. For the intermediate flux planes, the model simulated flux values were tabulated and compared to the experimentally calculated values in Table 3. Recall that steady-state conditions are assumed, but because the study is based upon actual measured concentrations within a three-dimensional aquifer model contaminant concentrations (and the corresponding flux values) may differ slightly from day to day simply due to minor variations in system conditions. For this reason data from two separate days (days 44 and 58) were used to demonstrate that the steady-state assumption was justified. All of the model-simulated results compared well with the experimentally calculated values. The largest percent difference was 11% at location x = 1.1 m, y = 0.25 m, and z = 0.65 m for both days 44 and 58. The mean absolute error was 0.017 mg/(cm^{2}day). It should be noted that the coupled SA-MRE algorithm provided results similar to an independent MRE algorithm while converging 5 times faster. All simulations were performed using a standard PC with a 2.8 MHz processor.

For the flux plane located at the downgradient edge of the source zone (x = 0.8 m) the model simulated flux values are listed in Table 4. The simulated flux values were verified by comparison to the effective PCE solubility range determined using Raoult's law (eq 1) and a pure phase PCE

solubility range of 150−200 mg/L. As discussed previously, the resulting effective PCE solubility range is 105−140 mg/L, which corresponds to an expected experimental range for the PCE flux of 1.07−1.43 mg/(cm^{2}day). It can be seen in Table 4 that each of the model simulated flux intensities compares well with the calculated effective flux range, with only location $x = 0.8$ m, $y = 0.3$ m, and $z = 0.60$ m barely exceeding the expected range (1.44 mg/(cm^{2}day)).

The SA-MRE simulated flux distribution for day 44 is shown in Figure 3a. For comparison, the observed source zone distribution recorded during excavation is displayed in Figure 3b. The excavation data are represented as a scatter plot, where each point represents an element within the source zone as determined from digital excavation images. The color of each element corresponds to the recorded red pixel intensity in the digital images.

The simulated flux distribution at the source plane (Figure 3a) compares well with the excavation source distribution (Figure 3b). It should be noted that the source located at $y = 0.15$ m, $z = 0.45$ m is not detected. This draws attention to a critical relationship between the transverse dispersivity and the downgradient sampling strategy. It is known that NAPL solution was injected at location $y = 0.15$ m, $z = 0.45$ m, and yet the model did not predict any significant mass flux at this location. The cause for this error is two-fold: there were no concentration observations within the direct downgradient path of the source zone in this region, and the transverse dispersivity of the system ($\alpha_T = 0.0002$ m) is relatively low. This indicates that even with the extensive data collected within the aquifer model, a known source was not detected due to the order of magnitude of the transverse dispersivity and the downgradient sampling strategy. However, results at all other locations demonstrate that the model performs well if the sampling strategy is established to take into account the scale of dispersion within the system.

As discussed previously, one of the benefits of applying the coupled SA-MRE model is that it provides estimates of the reliability associated with each of the model simulated flux values. Figure 4 shows the estimated 95% confidence limits for the intermediate flux plane located at $x = 1.1$ m, and the source plane $x = 0.8$ m. For both planes, all simulated mean flux values greater than 0.01 mg/(cm^2 day) are shown sorted in descending order with their corresponding 95% confidence interval. The flux values not shown in the figure (below 0.01 (mg/cm^2 day)) represent PCE flux in the region outside of the observed PCE plume. Each of the model simulated flux values below 0.01 mg/(cm^2 day) had a 95% confidence interval of 0.0−0.03 mg/(cm^2 day) which indicates a high confidence that the PCE flux at these locations is essentially zero. These values were not shown in the figure in order to focus attention on the model-simulated values displaying greater uncertainty (larger confidence intervals).

The simulated flux values greater than 1.0 mg/(cm^2 day) represent locations that were at or near the center of the PCE plume, while values below 0.5 mg/(cm^2 day) represent locations that were at the lateral extents of the plume. Figure 4 demonstrates that as we move from the farthest intermediate flux plane ($x = 1.1$ m) toward the source plane ($x = 0.8$ m) the reliability typically increases (the 95% confidence intervals decrease) for the flux estimates located at the center of the plume and that the lateral extent of PCE flux (width of the plume) decreases. These results follow the trend that we would expect to see as we move upgradient toward the source zone.

NAPL Source Zone Characterization. The hybrid SA-MRE method was applied in conjunction with a flux plane model to develop a tool for characterizing NAPL source zones in terms of mass flux. The coupled SA-MRE algorithm utilizes the robust search capabilities of SA while providing the ability to estimate the uncertainty associated with each of the simulated flux values more readily than an independent MRE algorithm. In its current form, the flux plane model is admittedly a simplification of a more complex problem and is only applicable under the conditions assumed for this study (uniform horizontal flow with advective-dispersive transport in a homogeneous aquifer and steady-state dissolution). The model provides a simple method for estimating the magnitude and spatial distribution of NAPL mass flux based upon observed aqueous phase concentrations. One possible application is that the flux plane model could be used to estimate the integrated mass flux or total mass crossing a specified boundary, such as a regulatory boundary or the intersection of adjoining properties. The method can be modified to incorporate different transfer functions and would be especially applicable if utilized with directly measured contaminant flux values obtained using a method such as that presented by Hatfield et al. (*36*).

Acknowledgments

Portions of this research were funded by the Natural and Accelerated Bioremediation Research (NABR) program, Biological and Environmental Research (BER), U.S. Department of Energy (Grant Number DE-FG02-97ER62471), the Florida Water Resources Center under a grant from the U.S. Department of Interior (Grant Number 01HQGR0138), and the Environmental Security Technology Certification (ESTCP) program, U.S. Department of Defense (DoD) (Project Number CU-0114). This paper has not been subject to DoD review and accordingly does not necessarily reflect the views of DoD.

Literature Cited

(1) Gorelick, S. M.; Evans, B.; Remson, I. Identifying sources of groundwater pollution: an optimization approach. *Water Resour. Res.* **1983**, *19* (3), 779−790.
(2) Aral, M. M.; Guan, J. Genetic algorithms in search of groundwater pollution sources. In *Advances in groundwater pollution control and remediation*. Aral, M. M., Ed.; NATO ASI Series; Kluwer Academic Publishers: Dordrecht, The Netherlands, 1996; pp 347−369.
(3) Atmadja, J.; Bagtzoglou, A. C. Pollution source identification in heterogeneous porous media. *Water Resour. Res.* **2001**, *37* (8), 2113−2125.
(4) Frind, E. O.; Molson, J. W.; Schirmer, M.; Guiguer, N. Dissolution and mass transfer of multiple organics under field conditions: The borden emplaced source. *Water Resour. Res.* **1999**, *35* (3), 683−694.
(5) Mahar, P. S.; Datta, B. Identification of pollution sources in transient groundwater systems. *Water Resour. Manage.* **2000**, *14*, 209−227.
(6) Mahar, P. S.; Datta, B. Optimal identification of ground-water pollution sources and parameter estimation. *J. Water Resour. Planning Manage.* **2001**, *127* (1), 20−29.
(7) McLaughlin, D.; Reid, L. B.; Li, S.-G.; Hyman, J. A stochastic method for characterizing groundwater contamination. *Ground Water* **1993**, *31* (2), 237−249.
(8) Sciortino, A.; Harmon, T. C.; Yeh, W. W-G. Inverse modeling for locating dense nonaqueous pools in groundwater under steady flow conditions. *Water Resour. Res.* **2000**, *36* (7), 1723−1735.
(9) Sciortino, A.; Harmon, T. C.; Yeh, W. W-G. Experimental design and model parameter estimation for locating a dissolving dense nonaqueous phase liquid pool in groundwater. *Water Resour. Res.* **2002**, *38* (5), 15-1 − 15-10.
(10) Sidauruk, P.; Cheng, A.H.-D. and Ouazar, D. Groundwater contamination source and transport parameter identification by correlation coefficient optimization. *Ground Water* **1998**, *36* (2), 208−214.
(11) Skaggs, T. H.; Kabala, Z. J. Recovering the release history of a groundwater contaminant. *Water Resour. Res.* **1994**, *30* (1), 71−80.
(12) Wagner, B. J. Simultaneous parameter estimation and contaminant source characterization for coupled groundwater flow and contaminant transport modelling. *J. Hydrol.* **1992**, *135* (1−4), 275−303.
(13) Rao, P. S. C.; et al. *Technology integration for contaminant site remediation: cleanup goals and performance criteria. Groundwater Quality: Natural and Enhanced Restoration of Ground-*

water Pollution, Proceedings of the Groundwater Quality 2001 Conference held at Sheffield, UK, IAHS Publication: 2001; Vol. 275, pp 571− 578.
(14) Lee, K. Y.; Chrysikopoulos, C. V. Numerical modeling of three-dimensional contaminant migration from dissolution of multicomponent NAPL pools in saturated porous media. *Environ. Geol.* **1995**, *26*, 157−165.
(15) Chrysikopoulos, C. V.; Lee, K. Y. Contaminant transport resulting from multicomponent nonaquesous phase liquid pool dissolution in three-dimensional subsurface formations. *J. Contam. Hydrol.* **1998**, *31*, 1−21.
(16) Chrysikopoulos, C. V.; Vogler, E. T. Acoustically enhanced multicomponent NAPL ganglia dissolution in water saturated packed columns. *Environ. Sci. Technol.* **2004**, *38*, 3940−2945.
(17) King, M. W. G.; Barker, J. F. Migration and natural fate of a coal tar creosote plume 1. Overview and plume development. *J. Contam. Hydrol.* **1999**, *39*, 249−279.
(18) Lee, K. Y.; Chrysikopoulos, C. V. Dissolution of a multicomponent DNAPL pool in an experimental aquifer. *J. Hazard. Mater.* **2006**, *B128*, 218−226.
(19) Rivett, M. O.; Feenstra, S.; Cherry, J. A. Transport of a dissolved phase plume from a residual solvent source in a sand aquifer. *J. Hydrol.* **1994**, *159*, 27−41.
(20) Rivett, M. O.; Feenstra, S.; Cherry, J. A. A controlled field experiment on groundwater contamination by multicomponent DNAPL: creation of the emplaced-source and overview of dissolved plume development. *J. Contam. Hydrol.* **2001**, *49*, 111−149.
(21) Newman, M. A.; K.; Hatfield, J. S.; Hayworth, P. S. C.; Rao, T. B.; Stauffer. A hybrid method for inverse characterization of subsurface contaminant flux. *J. Contam. Hydrol.* **2005**, *81* (1−4), 34−62.
(22) Newman M. A. Inverse Characterization of Subsurface Contaminant Mass Flux: A Three-dimensional Physical and Numerical Modeling Study, Ph.D. Dissertation, University of Florida, Gainesville, FL, 2001; pp 1−149.
(23) Pankow, J. F.; Cherry, J. A. *Dense Chlorinated Solvents and other DNAPLS in groundwater*; Waterloo Press: Portland, 1996.
(24) Lesage, S.; Brown, S. Observation of the dissolution of NAPL mixtures. *J. Contam. Hydrol.* **1994**, *15*, 57−71.
(25) Mabey, W. R.; Smith, J. H.; Podoll, R. T.; Johnson, H. L.; Mill, T.; et al. *Aquatic fate process data for organic priority pollutants*; Report No. 440/4-81-014; United States Environmental Protection Agency: Washington DC, 1982.
(26) Al-Raoush, R. I.; Willson, C. S. A pore-scale investigation of a multiphase porous media system. *J. Contam. Hydrol.* **2005**, *77*, 67−89.
(27) Domenico, P. A.; Robbins, G. A. A new method of contaminant plume analysis. *Ground Water* **1985**, *23* (4), 476−485.
(28) Kirkpatrick, S.; Gelatt, C. D.; Vecchi, M. P. Optimization by simulated annealing. *Science* **1983**, *220*, 671−680.
(29) Laarhoven, P. J. M.v.; Aarts, E. H. L. *Simulated annealing: theory and applications*; D. Reidel Publishing Company: Dordrecht, Holland, 1987.
(30) Press, W. H.; Teukolsky, S. A.; Vetterling, W. T.; Flannery, B. P. *Numerical recipes in FORTRAN: the art of scientific computing*; Cambridge University Press: Cambridge, 1992.
(31) Zheng, C.; Wang, P. Parameter structure indentification using tabu search and simulated annealing. *Adv. Water Resour.* **1996**, *19* (4), 215−224.
(32) Woodbury, A. D.; Ulrych, T. J. Minimum relative entropy: forward probabilistic modeling. *Water Resour. Res.* **1993**, *29* (8), 2847−2860.
(33) Woodbury, A. D.; Ulrych, T. J. Minimum relative entropy inversion: Theory and application to recovering the release history of a groundwater contaminant. *Water Resour. Res.* **1996**, *32* (9), 2671−2681.
(34) Woodbury, A. D.; Ulrych, T. J. Minimum relative entropy and probabilistic inversion in groundwater hydrology. *Stochastic Hydrol. Hydraulics* **1998**, *12*, 317−358.
(35) Woodbury, A.; Sudicky, E.; Ulrych, T. J.; Ludwig, R. Three-dimensional plume source reconstruction using minimum relative entropy inversion. *J. Contam. Hydrol.* **1998**, *32* (1−2), 131−158.
(36) Hatfield, K.; Annable, M.; Cho, J.; Rao, P. S. C.; Klammler, H. A direct passive method for measuring water and contaminant fluxes in porous media. *J. Contam. Hydrol.* **2004**, *75*, 155−181.

Received for review February 23, 2006. Revised manuscript received July 9, 2006. Accepted July 18, 2006.

ES060437S